Biochimica et Biophysica Acta 1812 (2011) 1607–1615

Contents lists available at SciVerse ScienceDirect

Biochimica et Biophysica Acta

journal homepage: www.elsevier.com/locate/bbadis

Severe dysfunction of respiratory chain and cholesterol metabolism in Atp7b$^{-/-}$ mice as a model for Wilson disease

Sven W. Sauer [a,*,1], Uta Merle [b,1], Silvana Opp [a], Dorothea Haas [a], Georg F. Hoffmann [a], Wolfgang Stremmel [b,1], Jürgen G. Okun [a,1]

[a] Department of Pediatrics, University Hospital, Heidelberg, Germany
[b] Department of Gastroenterology, University Hospital, Heidelberg, Germany

ARTICLE INFO

Article history:
Received 4 April 2011
Received in revised form 26 August 2011
Accepted 29 August 2011
Available online 2 September 2011

Keywords:
Wilson disease
Copper
Respiratory chain
Sterol metabolism
ROS

ABSTRACT

Wilson disease (WD) is caused by mutations of the WD gene ATP7B resulting in copper accumulation in different tissues. WD patients display hepatic and neurological disease with yet poorly understood pathomechanisms. Therefore, we studied age-dependent (3, 6, 47 weeks) biochemical and bioenergetical changes in *Atp7b*$^{-/-}$ mice focusing on liver and brain. Mutant mice showed strongly elevated copper and iron levels. Age-dependently decreasing hepatic reduced glutathione levels along with increasing oxidized to reduced glutathione ratios in liver and brain of 47 weeks old mice as well as elevated hepatic and cerebral superoxide dismutase activities in 3 weeks old mutant mice highlighted oxidative stress in the investigated tissues. We could not find evidence that amino acid metabolism or beta-oxidation is impaired by deficiency of ATP7B. In contrast, sterol metabolism was severely dysregulated. In brains of 3 week old mice cholesterol, 8-dehydrocholesterol, desmosterol, 7-dehydrocholesterol, and lathosterol were all highly increased. These changes reversed age-dependently resulting in reduced levels of all previously increased sterol metabolites in 47 weeks old mice. A similar pattern of sterol metabolite changes was found in hepatic tissue, though less pronounced. Moreover, mitochondrial energy production was severely affected. Respiratory chain complex I activity was increased in liver and brain of mutant mice, whereas complex II, III, and IV activities were reduced. In addition, aconitase activity was diminished in brains of *Atp7b*$^{-/-}$ mice. Summarizing, our study reveals oxidative stress along with severe dysfunction of mitochondrial energy production and of sterol metabolism in *Atp7b*$^{-/-}$ mice shedding new light on the pathogenesis of WD.

1. Introduction

Wilson disease (WD) is an autosomal recessive disorder caused by mutations of the WD gene ATP7B encoding for a copper transporting P-type ATPase [1]. Due to the deficient transporter copper excretion into the bile is impaired and it accumulates in liver and other organs, e.g. the brain, resulting in progressive clinical manifestations [2]. WD patients may suffer from liver disease, neurological or psychiatric abnormalities, or various combinations of these symptoms [3,4]. The mechanisms underlying the pathophysiology of WD are not well understood. Established animal models for WD are the Long Evans Cinnamon rat [5], the toxic milk mouse [6], and the *Atp7b*$^{-/-}$ mouse [7–9], all showing hepatic copper accumulation. However, cerebral damage has not yet been described in these animal models. With regard to the liver it has been proposed that free radical generation by excess copper and subsequent oxidative changes of organellar lipids and thiol-containing proteins in hepatocytes accounts for the development and progression of liver damage [10–12]. In line with this notion chronic copper exposure dramatically altered proteins involved in anti-oxidant defense in HepG2 cells [13,14]. A study of Gu and colleagues [15] in liver samples from affected patients indicated severe dysfunction of enzymes of mitochondrial energy production. Whether this was cause or consequence of liver damage remained unclear. Recently, a study in *Atp7b*$^{-/-}$ mice indicated imbalance of cholesterol metabolism [16].

To enhance the pathophysiological understanding of WD we studied the biochemical and bioenergetical phenotype of *Atp7b*$^{-/-}$ mice. As marker for oxidative stress Mn-dependent and Cu/Zn-dependent

Abbreviations: 7-DHC, 7-Dehydrocholesterol; 8-DHC, 8-Dehydrocholesterol; ESI-MS/MS, Electrospray ionization tandem mass spectrometry; Nitroso-PSAP, 2-Nitroso-5-(N-propyl-3-sulfopropylamino)phenol; ROS, Reactive oxygen species; SOD, Superoxide dismutase; WD, Wilson Disease

* Corresponding author at: University Children's Hospital, Department of General Pediatrics, Division of Inherited Metabolic Diseases, Im Neuenheimer Feld 430, D-69120 Heidelberg, Germany. Tel.: +49 6221 56 1776; fax: +49 6221 56 5565.
E-mail address: sven.sauer@med.uni-heidelberg.de (S.W. Sauer).

[1] Authors contributed equally.

0925-4439/$ – see front matter © 2011 Elsevier B.V. All rights reserved.
doi:10.1016/j.bbadis.2011.08.011

superoxide dismutase as well as glutathione content was measured. For biochemical characterization amino acid and acylcarnitine profile as well as metabolites of cholesterol biosynthesis were analyzed. To study the bioenergetical phenotype of *Atp7b*$^{-/-}$ mice, we measured enzyme complexes of the respiratory chain and aconitase.

2. Materials and methods

2.1. Animals

The generation of *Atp7b*$^{-/-}$ mice has been described previously [7]. *Atp7b*$^{-/-}$ mice (with a genetic 129/Sv background) and wild type 129/Sv mice were housed at the University of Heidelberg according to the guidelines of the Institutional Animal Care and Use Committees and in accordance with governmental requirements. *Atp7b*$^{-/-}$ and wild type mice at ages of 3, 6 weeks and 47 weeks were used for the experiments (7 animals per group). Mice were kept on a 12 h:12 h light: dark cycle. Food (normal chow diet containing 176 μg/g iron and 16 μg/g copper) and water were provided ad libitum. Animals were anesthetized with ketamine/xylazine. Blood was collected by cardiac puncture under anesthesia and afterwards animals were systematically perfused with saline from the left ventricle after thoracotomy to remove whole blood from organs. Subsequently tissues were removed and samples *were* stored at −80 °C.

2.2. Preparation of tissue homogenates

Tissues (brain and liver) were homogenized with a Potter Elvehjem system in a buffer containing 250 mmol/L sucrose, 50 mmol/L KCl, 5 mmol/L $MgCl_2$, 20 mmol/L Tris/HCl (adjusted at pH 7.4). Protein was determined according to Lowry [17] with the modifications of Helenius and Simons [18] using bovine serum albumin as a standard.

2.3. Measurement of iron-metabolism parameters

Tissue iron and copper quantification using atomic absorption spectroscopy was performed as described previously [19]. Iron and copper concentrations of tissues (μg/g of wet tissue) were calculated from the results of this analysis. The Ferrozin method was employed to quantify serum iron levels (AU 640, Olympus Diagnostics, Hamburg, Germany). In acidic environment, binding of reduced iron to [2,4,6-Tri-(2-Pyridyl)-5-Triazin] results in a blue colored complex, which is measured in a dual wavelength mode (600–800 nm).

2.4. Cu/Zn- and Mn-dependent superoxide dismutase

Cu/Zn- and Mn-dependent superoxide dismutase (SOD) activities were determined using a SOD assay kit (Cayman Chemical, Ann Arbor, U.S.A.) according to the manufacturer's protocol. In brief, tissue homogenates were centrifuged for 10 min at 600×*g* and 4 °C. The supernatant was centrifuged for 10 min at 3.500×*g* and 4 °C. The resulting cytosolic and mitochondrial fractions were used to assay Cu/Zn- and Mn-SOD respectively. The mitochondrial pellet was sonicated to disrupt membranes. To further differentiate between cytosolic and mitochondrial SOD, Cu/Zn- and Mn-SOD was inhibited by the addition of 3 mM potassium cyanide.

2.5. Glutathione content

Glutathione contents were assayed in tissue homogenates as previously described [20] with modifications. Tissue homogenates were

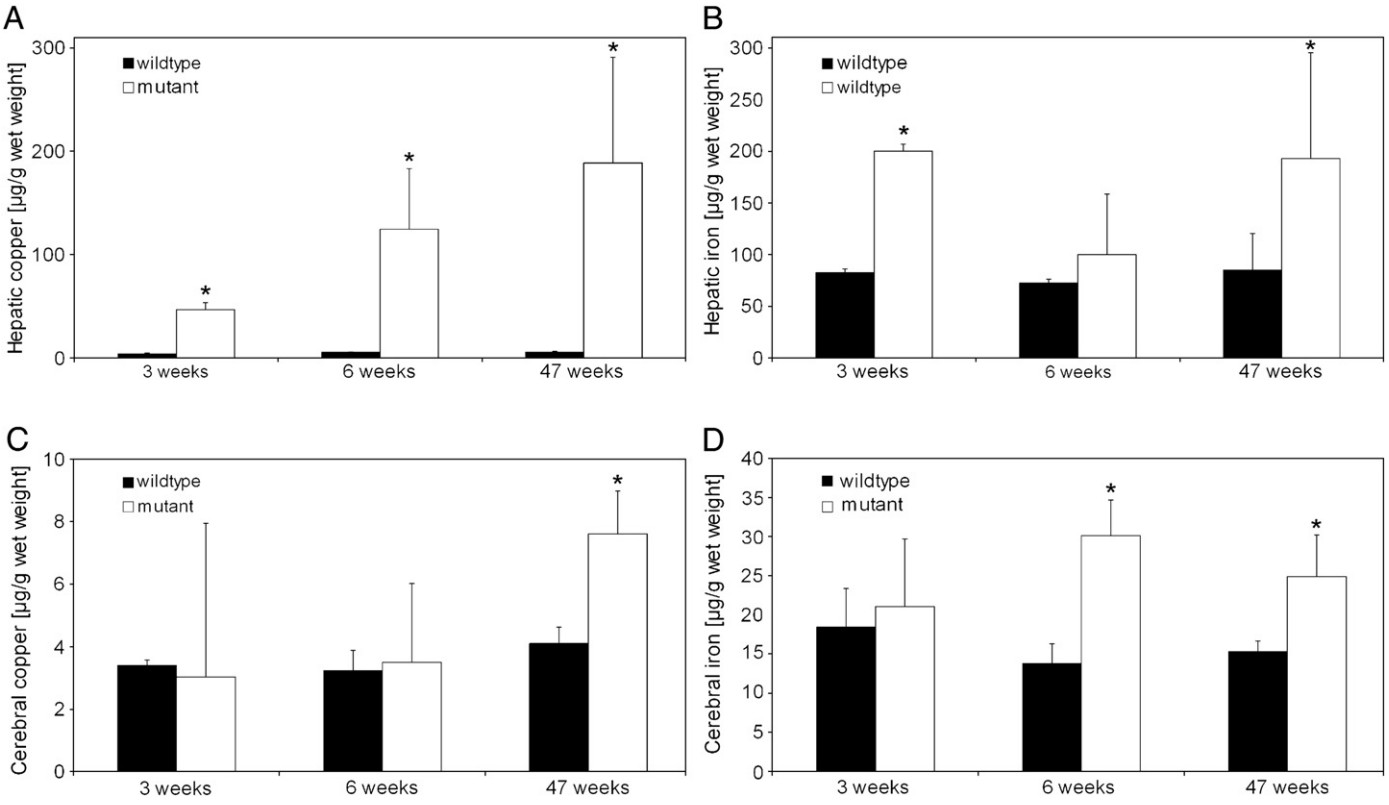

Fig. 1. *Hepatic and cerebral iron and copper contents. Atp7b*$^{-/-}$ mice displayed elevated hepatic copper and, in addition, iron levels. In liver copper levels (A) age-dependently increased and iron levels (B) were elevated in 3 and 47 week old mice. Cerebral copper contents (C) were elevated in 47 week old mice and iron levels (D) in 6 and 47 week old mice. Data are expressed as mean ± SD in μg/g wet weight (n = 7 mice per group; * $p<0.05$).

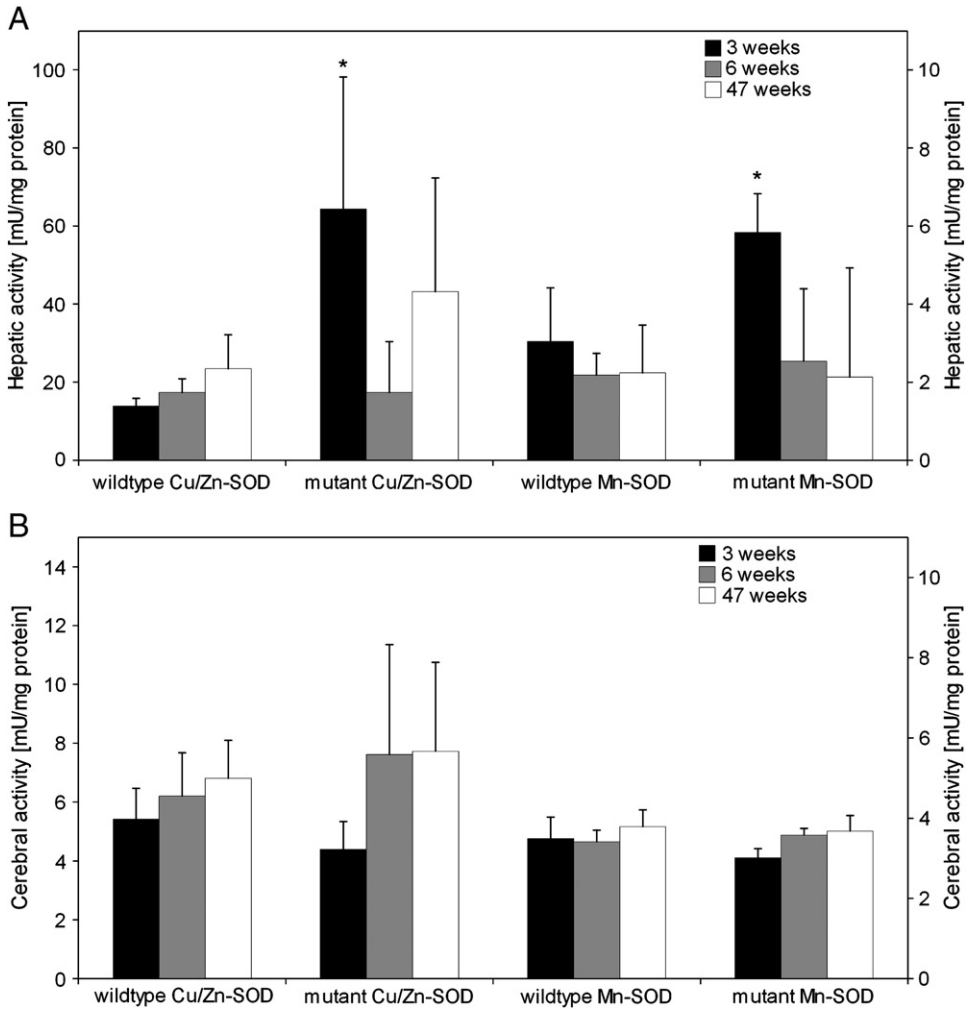

Fig. 2. *Activities of Cu/Zn- and Mn-dependent SOD.* Cu/Zn- and Mn-dependent SOD were assayed in liver (A) and brain (B) tissue homogenates of *Atp7b*$^{-/-}$ and wild type mice. Hepatic activity of both enzymes was increased in 3 week old mutant mice. In liver of older mice and in brain of all age groups activities were unchanged compared to wildtype mice. Data are expressed as mean ± SD in mU/g protein (n = 7 mice per group;* $p<0.05$).

centrifuged for 10 min at 600×*g* and 4 °C. The supernatant was deproteinized by addition of 0.5 volumes of sulfosalicylic acid (5%) and incubated for 30 min on ice. Afterwards, the samples centrifuged for 10 min at 1000*g and 4 °C. The pH of supernatants was increased by the addition of 50 µL triethanolamine (4 M) per mL sample. To measure GSH/GSSG ratio one part of the samples was derivatized with 10 µL 2-vinlypyridine (1 M) per mL of sample. GSH and GSSG content was detected as absorbance change at 410 nm that was correlated to a calibration curve and normalized to the protein content.

2.6. Quantitative analysis of acylcarnitines and amino acids

Acylcarnitines and amino acids were determined in tissue homogenates by electrospray ionization tandem mass spectrometry (ESI-MS/MS) according to a modified method as previously described [21] using a Quattro Ultima triple quadrupole mass spectrometer (Micromass, Manchester, UK) equipped with an electrospray ion source and a Micromass MassLynx data system.

2.7. Sterol analysis in tissue samples

After preparation of liver and brain homogenates and protein determination a sample of 1 mg total protein dissolved in 1 ml water was hydrolyzed and extracted as previously described [22]. Subsequent differentiation and quantification of sterols were performed by gas chromatography/mass spectrometry [23].

2.8. Spectrophotometric analysis of single respiratory chain complexes I–V and aconitase

Steady state activities of respiratory chain complexes I–V and aconitase in tissue homogenates were recorded using a computer tunable spectrophotometer (Spectramax Plus Microplate Reader, Molecular Devices, Sunnyvale, California, U.S.A.) operating in the dual wavelength mode. Samples were analyzed in temperature-controlled 96-well plates in a final volume of 300 µL as previously described [20]. In brief, tissue homogenates were centrifuged for 10 min at 600×*g* and 4 °C. The resulting supernatant was centrifuged for 10 min at 3.500×*g* and 4 °C. The mitochondrial pellet was used for further enzymatic assays. The specificity of the enzymatic assays was validated by the addition of standard respiratory chain inhibitors (complex I: 2-n-decylquinazolin-4-yl-amine [1 µmol/L]; complex II: thenoyltrifluoroacetone [8 mmol/L]; complex III: antimycin A [1 µmol/L]; complex IV: NaCN [2 mmol/L]; complex V: oligomycin [80 µmol/L]).

2.9. Statistical analysis

Data are expressed as mean ± S.D. if not noted otherwise. For pair wise and multiple comparisons Mann Whitney *U* test and Kruskal–

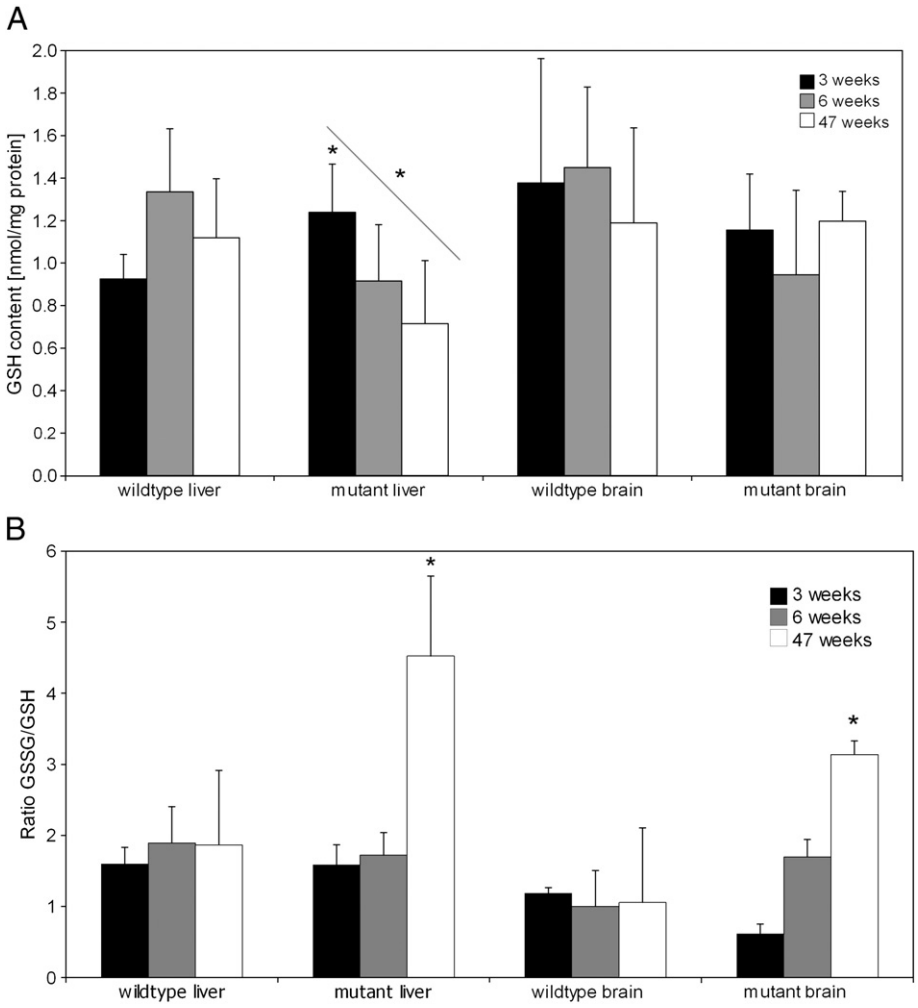

Fig. 3. *Glutathione content.* Cerebral glutathione content was not significantly changed in *Atp7b*$^{-/-}$ mice, whereas hepatic levels were significantly increased in 3 week old mutant mice. Hepatic glutathione levels were constantly decreasing over the age in mutant mice (A). In addition, oxidized to reduced glutathione (GSSG/GSH) ratios were highly elevated in liver and brain of 47 week old mice (B). Data are expressed as mean ± SD in nmol/mg protein (n = 7 mice per group;* $p<0.05$).

Wallis H test with Bonferroni adjustment respectively were calculated. Time-dependent changes were evaluated using ANOVA repeated measures. All statistics were calculated in SPSS for Windows 16.0 Software. $p<0.05$ was considered as significant.

3. Results

3.1. Elevated copper and iron levels in brain and liver

First we studied copper and iron content in liver and brain of *Atp7b*$^{-/-}$ mice. Mutant mice displayed strongly elevated hepatic copper and, in addition, iron levels. Copper levels age-dependently increased, whereas iron content was elevated in 3 and 47 week old mice. Copper levels in brain tissue were increased but only in 47 week old mice. Strikingly, the increase of cerebral iron content already occurred in 6 week old mice (Fig. 1).

3.2. Altered oxidative stress response

To evaluate oxidative stress in *Atp7b*$^{-/-}$ mice, we determined glutathione concentrations and SOD activity in liver and brain homogenates. Cu/Zn-dependent and Mn-dependent SOD activities were highly induced in the liver of 3 week old mutant mice, whereas unchanged in liver tissue of 6 week or 47 week old mice. Cerebral activities of both enzymes were similar in wild type and *Atp7b*$^{-/-}$ mice of all age groups (Fig. 2). Cerebral glutathione content did not differ between brain homogenates of mutant and wild type mice. In contrast, hepatic glutathione levels of 3 week old mutant mice were higher than in age-matched wild type mice. Further, glutathione levels were decreasing in mutant mice over the age, whereas similar glutathione concentrations were found in wild type mice of all age groups (Fig. 3A). Moreover, 47 week old mice showed highly increased oxidized to reduced glutathione (GSSG/GSH) ratios in liver and brain (Fig. 3B).

3.3. Increase of alanine content as marker of oxidative stress

Next, we studied whether amino acid metabolism was affected in mutant mice determining amino acid concentrations in liver and brain tissue as well as in serum of mutant and wild type mice. 3 week old mutant mice showed reduced concentrations of L-alanine in liver tissue, whereas 6 and 47 week old mutant mice displayed increased hepatic levels. Noteworthy, L-alanine is a marker for mitochondrial dysfunction [24]. Other amino acids were unchanged in mutant mice (Table 1).

Table 1
Amino acid contents in liver, brain and serum of wild type and mutant mice. Data are presented as mean in nmol/mg protein (liver, brain) and μM (serum; n = 7 mice per group;* $p<0.05$).

Weeks of age	Liver						Brain						Serum					
	Wild type			Mutant			Wild type			Mutant			Wild type			Mutant		
	3	6	47	3	6	47	3	6	47	3	6	47	3	6	47	3	6	47
Alanine	2494.79	1895.85	1551.39	**1206.83***	**3696.92***	**5619.45***	4087.98	3133.51	2768.05	4273.99	3563.63	2546.13	386.80	225.28	211.50	475.91	302.15	238.43
Valine	460.22	252.34	152.33	199.51	475.37	251.74	457.56	436.53	783.39	272.74	582.14	518.04	104.87	82.18	102.93	111.64	94.82	95.39
Leucine / Isoleucine	265.38	246.06	206.97	246.07	325.20	203.70	731.24	788.11	1342.22	568.08	827.52	926.53	123.96	89.13	121.85	136.25	112.32	106.48
Methionine	92.98	90.74	154.00	68.31	199.24	124.13	310.21	318.25	552.73	189.30	287.63	350.84	39.53	32.51	39.32	50.38	41.65	34.91
Phenylalanine	98.85	109.78	126.30	95.06	105.27	152.73	397.60	391.08	732.51	253.17	348.29	453.43	55.80	34.56	40.09	54.03	41.23	39.20
Tyrosine	69.28	80.18	85.71	89.26	83.13	88.66	275.57	218.77	523.78	176.63	228.60	356.59	47.96	38.75	45.40	65.10	46.55	51.21
Glutamic acid	5956.19	6076.16	7200.84	5099.25	5975.53	5676.23	212.91	299.32	960.42	169.35	179.61	1084.84	117.87	94.55	92.37	137.89	110.01	106.59
Tryptophan	717.57	807.22	859.23	627.41	720.30	697.36	57.06	67.42	175.79	41.71	47.48	153.64	56.14	44.81	42.57	50.12	38.27	39.38
Proline	6639.25	1936.81	1868.09	1689.71	3241.63	1953.68	2186.97	3609.58	7626.65	1854.35	4360.26	5218.64	254.04	154.54	167.46	447.61	200.84	169.97
Histidine	966.64	1027.17	1518.29	1106.07	2371.35	1632.98	709.71	450.42	1001.31	720.06	105.52	550.44	132.47	100.85	132.60	143.15	116.23	128.67
Threonine	1084.18	301.78	300.67	308.45	520.16	441.53	564.14	506.64	929.50	381.04	613.29	564.46	73.13	68.30	72.10	98.70	74.22	54.24
Glycine	1341.94	1312.80	1513.70	1230.36	1315.83	1421.21	2312.34	1993.88	2419.34	1559.05	1893.19	2364.49	168.10	157.53	112.47	290.82	173.03	164.08
Ornithine	4.34	3.93	3.75	4.31	3.04	3.65	87.70	80.97	120.78	55.00	67.53	86.30	5.02	3.67	3.60	5.35	3.46	4.93
Arginine	546.99	623.83	794.15	561.01	661.56	865.53	10.76	5.93	12.07	8.26	7.13	8.28	153.01	100.50	115.01	171.08	112.79	65.41
Citrulline	27.34	24.38	34.94	25.67	23.15	23.35	43.33	34.16	33.55	29.34	36.64	45.23	32.95	27.02	32.46	49.60	35.98	28.18
Aginino succinic acid	23.20	23.33	33.05	19.59	19.40	24.53	12.92	5.85	6.36	4.50	4.18	3.99	0.31	0.14	0.15	0.26	0.16	0.13
Homocitrulline	8.80	8.52	8.28	7.68	7.83	8.24	9.34	8.59	18.57	5.09	5.52	6.39	2.04	2.26	2.01	2.99	2.50	2.34

3.4. No abnormalities in beta-oxidation

Acylcarnitine profiling is a well established method to study beta-oxidation defects. Changes in the profile are like fingerprints for enzymatic defects in the mitochondrial fatty acid degradation. Free carnitine levels in liver and acetylcarnitine concentrations in serum were reduced in mutant mice of all tested age groups. Beside these findings, no major changes of beta-oxidation metabolites were found in liver, brain or serum of mutant mice suggesting unaffected beta-oxidation (Table 2).

3.5. Complex pattern of sterol metabolism dysregulation

A recent study indicated that *Atp7b*$^{-/-}$ mice display a disturbed cholesterol metabolism. Therefore, we measured different sterols in liver, brain, and serum of mutant compared to wild type mice. In brain homogenates several sterol metabolites revealed an intriguing pattern of concentration changes, in 3 week old mice cholesterol, 8-DHC, desmosterol, 7-DHC, and lathosterol were highly increased ranging from 1.6 to 4.7 fold. The high brain levels of these metabolites were decreasing in an age dependent way resulting in reduced cholesterol, desmosterol, and lathosterol concentrations in 6 week old mice and highly reduced levels of all previously increased sterol metabolites in 47 week old mice. The hepatic phenotype was less severe. Although the concentrations of all tested sterol metabolites were lower or decreasing over the age, only cholesterol was significantly reduced in 3 and 6 week old mice. In serum, cholesterol, cholestanol, 8-DHC, 7-DHC, and desmosterol were reduced in 47 week old mice (Fig. 4).

3.6. Impairment of mitochondrial energy metabolism

Oxidative damage induced by Fenton reaction is thought to play a major role in the pathophysiology of WD. The respiratory chain is a major source of ROS but also especially susceptible to oxidative damage. Therefore, we investigated the activity of respiratory chain single enzyme complexes in liver and brain homogenates. Strikingly, there was a time-dependent increase of complex I activity in liver and brain tissue. Complex II activity was reduced in the liver of 47 week old mice and in brain tissue independent of age. Hepatic complex III activity was decreased and complex IV activity was lower in liver and brain homogenates of 47 week old mutant mice. Complex V displayed a reduced activity in liver and brain of 3 and 6 week old mutant mice, 47 week old mice however were indistinguishable from wild type mice. Comparing only genotypes, *Atp7b*$^{-/-}$ mice display a common phenotype in liver and brain consisting of increased complex I and reduced complex III-V activities except for complex II which was only reduced in brain tissue (Fig. 5).

Aconitase is highly vulnerable for oxidative stress. Therefore, we analyzed aconitase activity in tissue homogenates. Hepatic activity was unchanged in mutant mice, whereas cerebral activity was lower in 3 and 6 week old *Atp7b*$^{-/-}$ mice compared to their wild type littermates (Fig. 6).

4. Discussion

WD patients display progressive hepatic and cerebral disease. The main biochemical finding is massive copper accumulation in affected tissue. The underlying pathomechanism of tissue damage, however, remains unknown. Copper accumulation has been suggested to induce ROS production by Fenton reaction leading to oxidative damage of proteins and lipids. To unravel the pathomechanism of WD, we biochemically and bioenergetically characterized *Atp7b*$^{-/-}$ mice. Corresponding to affected human individuals *Atp7b*$^{-/-}$ mice display highly elevated copper and, in addition, iron levels in liver and brain. We could show that hepatic GSH levels age-dependently decreased, whereas oxidized to reduced

Table 2
Acylcarnintine contents in liver, brain and serum of wild type and mutant mice C0, free carnitine; C2, acetylcarnitine; C3, propionylcarnitine; C4, butyrylcarnitine; C5:1, pentenoylcarnitine; C5, isovalerylcarnitine; C6, hexanoylcarnitine; C8:1, octenoylcarnitine; C8, octanoylcarnitine; C10:1, decenoylcarnitine; C10, decanoylcarnitine; C12, dodecanoylcarnitine; C14:1, tetradecenoylcarnitine; C14, tetradecanoylcarnitine; C14OH, hydroxytetradecanoylcarnitine; C16:1, hexadecenoylcarnitine; C16, palmitoylcarnitine; C16:1OH, hydroxyhexadecenoylcarnitine; C16OH, hydroxyhexadecanoylcarnitine; C18:1, octadecenoylcarnitine; C18, stearoylcarnitine; C18:1OH, hydroxyoctadecenoylcarnitine; C18OH, hydroxyoctadecanoylcarnitine; C18:2, octadecadienoylcarnitine. Data are presented as mean in nmol/mg protein (liver, brain) or μM (serum; n = 7 mice per group;* $p<0.05$).

Weeks of age	Liver						Brain						Serum					
	Wild type			Mutant			Wild type			Mutant			Wild type			Mutant		
	3	6	47	3	6	47	3	6	47	3	6	47	3	6	47	3	6	47
C0	46.56	44.08	44.39	26.93	25.70	30.29	79.33	90.33	72.74	68.93	64.15	77.59	18.17	16.09	17.45	**12.17***	**12.25***	**13.14***
C2	50.98	47.91	45.12	48.65	50.14	43.21	2.61	5.10	8.66	2.31	2.18	10.31	6.67	5.85	5.59	**3.89***	**2.99***	**2.91***
C3	0.30	0.26	0.21	0.24	0.23	0.14	0.44	0.37	0.22	0.26	0.24	0.16	0.19	0.09	0.27	0.13	0.09	0.08
C4	0.30	0.21	0.20	0.18	0.16	0.23	3.73	4.28	4.23	1.81	4.37	4.43	0.71	0.17	0.29	0.67	0.14	0.11
C5:1	0.15	0.24	0.30	0.09	0.13	0.33	0.06	0.16	0.08	0.08	0.05	0.06	0.03	0.01	0.01	0.01	0.01	0.01
C5	0.57	0.46	0.39	0.31	0.32	0.62	0.25	0.28	0.21	0.42	0.22	0.30	0.18	0.09	0.14	0.11	0.09	0.06
C6	0.13	0.10	0.19	0.08	0.16	0.08	0.09	0.11	0.05	0.09	0.08	0.05	0.08	0.03	0.02	0.05	0.02	0.01
C8:1	1.14	1.31	1.20	1.41	0.96	1.11	0.48	0.29	0.17	0.64	0.32	0.17	0.03	0.01	0.01	0.01	0.01	0.01
C8	0.04	0.07	0.06	0.00	0.05	0.00	0.04	0.05	0.15	0.07	0.08	0.04	0.04	0.01	0.01	0.02	0.01	0.01
C10:1	0.29	0.42	0.28	0.51	0.27	0.46	0.10	0.10	0.08	0.14	0.06	0.08	0.09	0.04	0.03	0.03	0.03	0.03
C10	0.05	0.09	0.05	0.13	0.14	0.07	0.06	0.08	0.09	0.07	0.07	0.03	0.10	0.03	0.02	0.03	0.02	0.02
C12	0.05	0.02	0.00	0.21	0.00	0.03	0.02	0.00	0.00	0.03	0.08	0.05	0.19	0.03	0.01	0.01	0.01	0.01
C14:1	0.09	0.11	0.05	0.09	0.06	0.05	0.08	0.04	0.03	0.07	0.09	0.04	0.02	0.05	0.02	0.01	0.02	0.02
C14	0.11	0.39	0.15	0.14	0.17	0.19	0.28	0.23	0.09	0.22	0.15	0.10	0.16	0.07	0.03	0.04	0.03	0.03
C14OH	0.20	0.23	0.19	0.28	0.24	0.14	0.32	0.16	0.14	0.22	0.13	0.11	0.13	0.02	0.02	0.01	0.01	0.01
C16:1	0.09	0.09	0.08	0.10	0.07	0.06	0.09	0.05	0.05	0.06	0.04	0.03	0.02	0.03	0.02	0.01	0.02	0.01
C16	0.19	0.26	0.33	0.25	0.31	0.22	0.11	0.18	0.17	0.11	0.11	0.09	0.12	0.16	0.08	0.08	0.10	0.07
C16:1OH	0.17	0.19	0.25	0.20	0.38	0.25	0.12	0.11	0.04	0.16	0.07	0.05	0.01	0.01	0.01	0.01	0.01	0.01
C16OH	0.47	0.46	0.47	0.60	0.51	0.34	0.14	0.15	0.12	0.19	0.10	0.10	0.01	0.02	0.01	0.01	0.01	0.01
C18:1	0.08	0.07	0.18	0.14	0.10	0.09	0.12	0.10	0.08	0.08	0.07	0.04	0.04	0.06	0.04	0.03	0.04	0.03
C18	0.28	0.26	0.29	0.34	0.20	0.23	0.16	0.15	0.09	0.13	0.11	0.10	0.06	0.05	0.03	0.04	0.04	0.03
C18:1OH	0.20	0.17	0.21	0.14	0.11	0.07	0.05	0.06	0.07	0.07	0.04	0.05	0.01	0.01	0.01	0.01	0.01	0.01
C18OH	0.33	0.42	0.40	0.47	0.26	0.32	0.15	0.20	0.08	0.22	0.12	0.11	0.02	0.01	0.01	0.01	0.01	0.01
C18:2	0.08	0.12	0.09	0.07	0.09	0.10	0.05	0.09	0.08	0.06	0.06	0.04	0.03	0.05	0.03	0.03	0.03	0.02

glutathione ratios in liver and brain of 47 week old mice increased. Further, superoxide dismutase activities in liver and brain of 3 week old mutant mice were up-regulated. Both findings clearly indicate production of ROS and altered anti-oxidative response. Mitochondrial respiratory chain is a well-known source and target of ROS. Accordingly, mitochondrial dysfunction and morphological abnormalities were described in liver from patients with WD [15,25]. Oxidative damage was found in liver of WD patients and in two rat models for WD, namely copper-loaded rats [26] and the Long-Evans Cinnamon rat model [27]. Noteworthy, the study of Gu and colleagues [15] provided evidence for decreased activities of respiratory chain complexes I–IV as well as of aconitase in liver tissue from 3 affected patients with deteriorating liver function and hepatic failure. The authors speculated that these changes may be induced either by direct oxidative damage of proteins or by depletion of mtDNA due to ROS. In such an advanced state of liver failure, however, it remains unclear whether respiratory chain dysfunction is a cause or consequence of degenerating hepatocytes. Furthermore, reduced complex II activity cannot be explained by mtDNA depletion since this protein is entirely nuclear-encoded. In line with the study of Gu and colleagues, *Atp7b*$^{-/-}$ mice display severe and age-dependent dysfunction of respiratory chain complexes in liver tissue. Since these mice do not develop hepatic failure, our data indicate that respiratory chain dysfunction is a direct consequence of Atp7 deficiency and contributes to the pathomechanism of WD. In contrast, complex I activity was age-dependently increased in mutant mice. This may represent a compensatory mechanism counteracting reduced respiratory chain function. Complex I is a major source of mitochondrial ROS production [28]. Its upregulation will induce increased production of ubiquinol that cannot fully be recycled due to diminished complex III activity ultimately leading to ROS production by reversed electron flow.

Neurological disease in WD is poorly understood, though severe damage of basal ganglia has been described [29]. Unfortunately, all available rodent models for WD do not display neurological disease. Interestingly, we could find changed cerebral activities of respiratory chain enzyme complexes similar to the liver phenotype and, in addition, a decrease of aconitase activity. Degeneration of basal ganglia is a common finding in inherited defects of mitochondrial energy production. Our findings could therefore point to an involvement of impaired respiratory chain function in the neuropathogenesis of WD.

In line with our findings Zischka and colleagues [30] showed in a rat model of WD that copper overload changes mitochondrial membrane integrity resulting in structural and functional impairment of mitochondria. Direct impairment of mitochondrial function by copper may represent an additional or alternative explanation to oxidative damage caused by Fenton reaction for the pathophysiology of WD.

A study of Huster and colleagues [16] showed reduced levels of cholesterol in serum of *Atp7b*$^{-/-}$ mice. mRNA levels of almost all proteins involved in cholesterol biosynthesis were down-regulated. However, sterol regulatory-binding protein 2 (SREBP-2), a transcription factor which activates cholesterol biosynthesis, was activated and correctly localized. The amount of mRNA for low density lipoprotein receptor (LDLR), which is directly controlled by SREBP-2 and would be expected to be up-regulated in response to elevated SREBP-2 was significantly reduced in *Atp7b*$^{-/-}$ mice and in human WD livers. Consequently, the authors speculated that SREBP-2 target genes but not SREBP-2 are dysregulated most likely due to an inhibition of SREBP-2 function by massive copper accumulation. Interestingly exposure of human macrophages to slightly elevated copper concentrations resulted in an increased expression of cholesterol biosynthesis genes [31]. Long-Evans Cinnamon rats display a similar biochemical phenotype including reduced cholesterol levels and a reduced activity of enzymes of sterol metabolism, namely 3-hydroxy-3-methylglutaryl coenzyme A reductase, cholesterol 7-alpha-hydroxylase, and acyl CoA: cholesterol acyltransferase [32]. In line with these studies, we found tremendous changes in sterol metabolism in tissues of *Atp7b*$^{-/-}$ mice. In liver samples cholesterol precursors 7-DHC, 8-DHC, lathosterol and

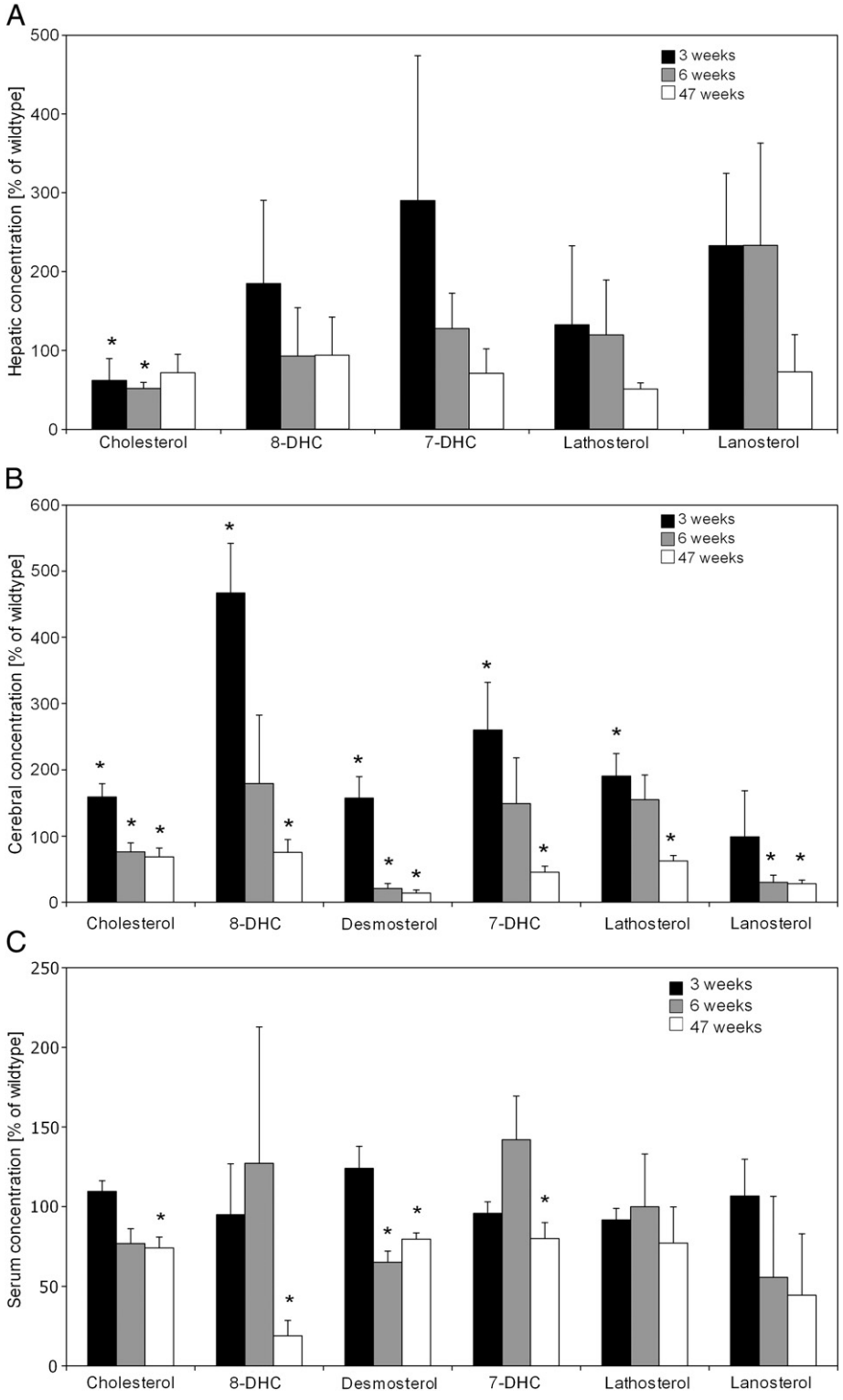

Fig. 4. *Sterol metabolism dysregulation.* We measured different sterol metabolites in liver (A), brain (B), and serum (C) of mutant and wild type mice. In brain of 3 week old mice cholesterol, 8-DHC, desmosterol, 7-DHC, and lathosterol were highly increased, whereas cholesterol, desmosterol, and lathosterol concentrations were reduced in 6 week and 47 week old mice. Hepatic cholesterol was also significantly reduced in 3 and 6 week old mice. In serum, cholesterol, 8-DHC, 7-DHC, and desmosterol were reduced in 47 week old mice. Data are presented as mean ± SD expressed as concentration in percent of the corresponding wild type littermates ($n = 7$ mice per group;* $p < 0.05$).

lanosterol were elevated in 3 week old mice. Cholesterol and all precursors decreased with age and were lower than in controls after 47 weeks of age. In brain of 3 week old mice all sterols were increased compared to controls. In 6 week old mice cerebral sterols declined with still moderate elevations of 7-DHC, 8-DHC and lanosterol. In 47 week old mice, who have clearly increased cerebral copper concentrations all sterols were significantly lower than in controls. These patterns may reflect significant difference in regulatory cell response to short-term

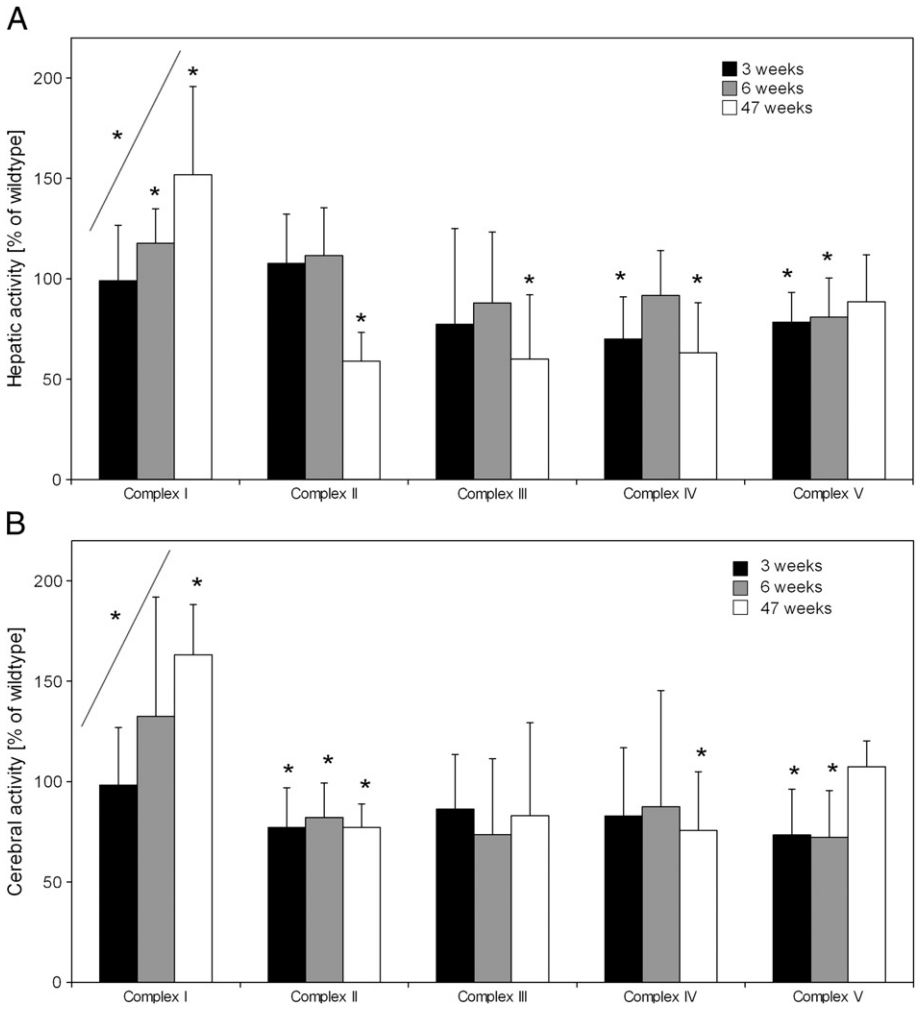

Fig. 5. *Activities of respiratory chain complexes.* We studied activities of respiratory chain single enzyme complexes in liver (A) and brain (B) homogenates. Complex I activity was increasing over the age in liver and brain tissue. In contrast, complex II activity was reduced in the liver of 47 week old mice and in brain tissue of all age groups. Complex III activity was decreased in the liver and complex IV activity was reduced in liver and brain homogenate of 47 week old mutant mice. Cerebral and hepatic complex V activity was diminished in liver and brain of 3 and 6 week old mutant mice. Data are presented as mean ± SD expressed as activity in percent of the corresponding wild type littermates ($n = 7$ mice per group;* $p < 0.05$).

mild copper elevation compared to prolonged exposure to toxic levels of copper.

Summarizing, *Atp7b*$^{-/-}$ mice display a pattern of oxidative stress along with severe dysfunction of mitochondrial energy production and of sterol metabolism. We hypothesize that these impairments cause liver disease and neurological abnormalities observed in WD.

References

[1] R.E. Tanzi, K. Petrukhin, I. Chernov, J.L. Pellequer, W. Wasco, B. Ross, D.M. Romano, E. Parano, L. Pavone, L.M. Brzustowicz, et al., The Wilson disease gene is a copper transporting ATPase with homology to the Menkes disease gene, Nat. Genet. 5 (4) (1993) 344–350.
[2] I.H. Scheinberg, I. Sternlieb, Wilson disease, in: L.H. Smith (Ed.), Major Problems in Internal Medicine, Saunders, Philadelphia, 1984, pp. 1–179.
[3] G. Loudianos, J.D. Gitlin, Wilson's disease, Semin. Liver Dis. 20 (2000) 353–364.
[4] E.A. Roberts, M.L. Schilsky, A practice guideline on Wilson disease, Hepatology 37 (2003) 1475–1492.
[5] J. Wu, J.R. Forbes, H.S. Chen, D.W. Cox, The LEC rat has a deletion in the copper transporting ATPase gene homologous to the Wilson disease gene, Nat. Genet. 7 (1994) 541–545.
[6] M.B. Theophilos, D.W. Cox, J.F. Mercer, The toxic milk mouse is a murine model of Wilson disease, Hum. Mol. Genet. 5 (1996) 1619–1624.
[7] O.I. Buiakova, J. Xu, S. Lutsenko, S. Zeitlin, K. Das, S. Das, B.M. Ross, C. Mekios, I.H. Scheinberg, T.C. Gilliam, Null mutation of the murine ATP7B (Wilson disease) gene results in intracellular copper accumulation and late-onset hepatic nodular transformation, Hum. Mol. Genet. 8 (1999) 1665–1671.
[8] D. Huster, M.J. Finegold, C.T. Morgan, J.L. Burkhead, R. Nixon, S.M. Vanderwerf, C.T. Gilliam, S. Lutsenko, Consequences of copper accumulation in the livers of the Atp7b$^{-/-}$ (Wilson disease gene) knockout mice, Am. J. Pathol. 168 (2006) 423–434.
[9] U. Merle, S. Tuma, T. Herrmann, V. Muntean, M. Volkmann, S.G. Gehrke, W. Stremmel, Evidence for a critical role of ceruloplasmin oxidase activity in iron metabolism of Wilson disease gene knockout mice, J. Gastroenterol. Hepatol. 25 (2010) 1144–1150.
[10] S.D. Aust, L.A. Morehouse, C.E. Thomas, Role of metals in oxygen radical reactions, J. Free Radic. Biol. Med. 1 (1985) 3–25.
[11] P. Hochstein, K.S. Kumar, S.J. Forman, Lipid peroxidation and the cytotoxicity of copper, Ann. N. Y. Acad. Sci. 355 (1980) 240–248.
[12] R.J. Sokol, D. Twedt, J.M. McKim Jr., M.W. Devereaux, F.M. Karrer, I. Kam, G. von Steigman, M.R. Narkewicz, B.R. Bacon, R.S. Britton, et al., Oxidant injury to hepatic mitochondria in patients with Wilson's disease and Bedlington terriers with copper toxicosis, Gastroenterology 107 (1994) 1788–1798.
[13] S. Strand, W.J. Hofmann, A. Grambihler, H. Hug, M. Volkmann, G. Otto, H. Wesch, S.M. Mariani, V. Hack, W. Stremmel, P.H. Krammer, P.R. Galle, Hepatic failure and liver cell damage in acute Wilson's disease involve CD95 (APO-1/Fas) mediated apoptosis, Nat. Med. 4 (1998) 588–593.
[14] I. Jimenez, P. Aracena, M.E. Letelier, P. Navarro, H. Speisky, Chronic exposure of HepG2 cells to excess copper results in depletion of glutathione and induction of metallothionein, Toxicol. In Vitro 16 (2002) 167–175.
[15] M. Gu, J.M. Cooper, P. Butler, A.P. Walker, P.K. Mistry, J.S. Dooley, A.H.V. Schapira, Oxidative-phosphorylation defects in liver of patients with Wilson's disease, Lancet 356 (2000) 469–474.
[16] D. Huster, T.D. Purnat, J.L. Burkhead, M. Ralle, O. Fiehn, F. Stuckert, N.E. Olson, D. Teupser, S. Lutsenko, High copper selectively alters lipid metabolism and cell cycle machinery in the mouse model of Wilson disease, J. Biol. Chem. 282 (2007) 8343–8355.
[17] O.H. Lowry, N.R. Roseborough, A.J. Farr, Protein measurement with the Folin phenol reagent, J. Biol. Chem. 193 (1951) 265–275.

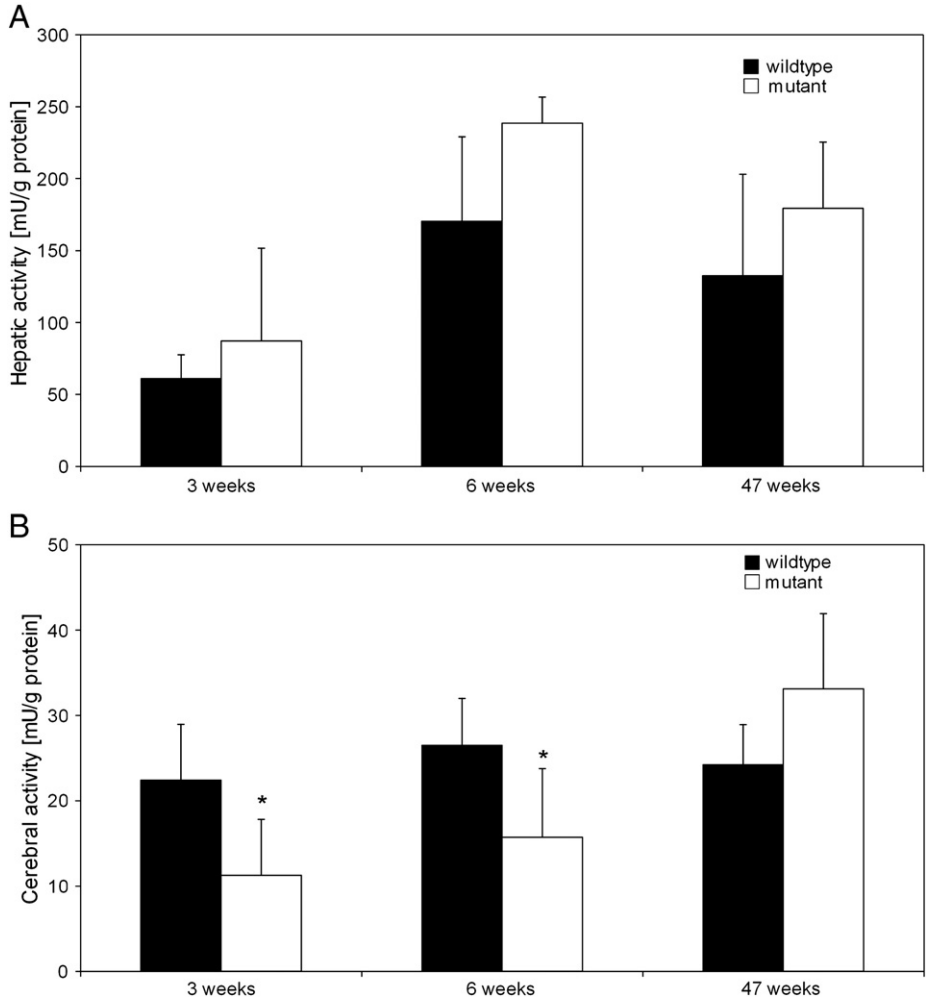

Fig. 6. *Aconitase activity.* Aconitase activity was analyzed in liver (A) and brain (B) tissue of *Atp7b*$^{-/-}$ and wild type mice. The enzymatic activity was unaffected in liver of mutant mice but was lower in brains of 3 and 6 week old *Atp7b*$^{-/-}$ mice. Data are presented as mean ± SD in mU/g protein (n = 7 mice per group;* $p<0.05$).

[18] A. Helenius, K. Simons, The binding of detergents to lipophilic and hydrophilic proteins, J. Biol. Chem. 247 (1972) 3656–3661.
[19] J.R. Nicholson, M.G. Savory, J. Savory, M.R. Wills, Micro-quantity tissue digestion for metal measurements by use of a microwave acid-digestion bomb, Clin. Chem. 35 (1989) 488–490.
[20] S.W. Sauer, J.G. Okun, M.A. Schwab, L.R. Crnic, G.F. Hoffmann, S.I. Goodman, D.M. Koeller, S. Kölker, Bioenergetics in glutaryl-coenzyme A dehydrogenase deficiency: a role for glutaryl-coenzyme A, J. Biol. Chem. 280 (2005) 21830–21836.
[21] S.W. Sauer, J.G. Okun, G. Fricker, A. Mahringer, I. Müller, L.R. Crnic, C. Mühlhausen, G.F. Hoffmann, F. Hörster, S.I. Goodman, C.O. Harding, D.M. Koeller, S. Kölker, Intracerebral accumulation of glutaric and 3-hydroxyglutaric acids secondary to limited flux across the blood-brain barrier constitute a biochemical risk factor for neurodegeneration in glutaryl-CoA dehydrogenase deficiency, J. Neurochem. 97 (2006) 899–910.
[22] C. Schmelzer, J.G. Okun, D. Haas, K. Higuchi, J. Sawashita, M. Mori, F. Döring, The reduced form of coenzyme Q10 mediates distinct effects on cholesterol metabolism at the transcriptional and metabolite level in SAMP1 mice, IUBMB Life 62 (2010) 812–818.
[23] D. Haas, J. Morgenthaler, F. Lacbawan, B. Long, H. Runz, S.F. Garbade, J. Zschocke, R.I. Kelley, J.G. Okun, G.F. Hoffmann, M. Muenke, Abnormal sterol metabolism in holoprosencephaly: studies in cultured lymphoblasts, J. Med. Genet. 44 (2007) 298–305.
[24] O. Shaham, N.G. Slate, O. Goldberger, Q. Xu, A. Ramanathan, A.L. Souza, C.B. Clish, K.B. Sims, V.K. Mootha, A plasma signature of human mitochondrial disease revealed through metabolic profiling of spent media from cultured muscle cells, Proc. Natl. Acad. Sci. U.S.A. 107 (2010) 1571–1575.
[25] I. Sternlieb, Mitochondrial and fatty changes in hepatocytes of patients with Wilson's disease, Gastroenterology 55 (1968) 354–367.
[26] R.J. Sokol, M. Devereaux, G.W. Mierau, K.M. Hambridge, R.H. Shikes, Oxidant injury to hepatic mitochondrial lipids in rats with dietary copper overload: modification by vitamin E deficiency, Gastroenterology 9 (1990) 1061–1071.
[27] J.M. McKim, M.W. Devereaux, R.D. Petersen, K.M. Hambidge, S.Z. Ruyle, M.L. Schilsky, I. Sternlieb, Mitochondrial oxidant injury in Long-Evans Cinnamon (LEC) rat liver containing high copper, Gastroenterology [abstract] 106 (1994) A941.
[28] W.J. Koopman, L.G. Nijtmans, C.E. Dieteren, P. Roestenberg, F. Valsecchi, J.A. Smeitink, P.H. Willems, Mammalian mitochondrial complex I: biogenesis, regulation, and reactive oxygen species generation, Antioxid. Redox Signal. 12 (2010) 1431–1470.
[29] L.K. Prashanth, S. Sinha, A.B. Taly, M.K. Vasudev, Do MRI features distinguish Wilson's disease from other early onset extrapyramidal disorders? An analysis of 100 cases, Mov. Disord. 25 (2010) 672–678.
[30] H. Zischka, J. Lichtmannegger, S. Schmitt, N. Jägemann, S. Schulz, D. Wartini, L. Jennen, C. Rust, N. Larochette, L. Galluzzi, V. Chajes, N. Bandow, V.S. Gilles, A.A. DiSpirito, I. Esposito, M. Goettlicher, K.H. Summer, G. Kroemer, Liver mitochondrial membrane crosslinking and destruction in a rat model of Wilson disease, J. Clin. Invest. 121 (2011) 1508–1518.
[31] P.A. Svensson, M.C.O. Englund, E. Markström, B.G. Ohlsson, M. Jarnas, H. Billig, J.S. Torgerson, O. Wiklund, L.M.S. Carlsson, B. Carlsson, Copper induces the expression of cholesterogenic genes in human macrophages, Atherosclerosis 169 (2003) 71–76.
[32] E. Levy, S. Brunet, F. Alvarez, E. Seidman, G. Bouchard, E. Escobar, S. Martin, Abnormal hepatobiliary and circulating lipid metabolism in the Long-Evans Cinnamon rat model of Wilson's disease, Life Sci. 80 (2007) 1472–1483.